Ultrahigh Strength and Stiffness in Cross-Linked Hierarchical Carbon Nanotube Bundles

*T. Filleter, R. Bernal, S. Li, and H.D. Espinosa**

Utilizing the full mechanical capabilities of individual carbon nanotubes (CNT) – which can exhibit tensile strength and elastic modulus of up to 1TPa and 100 GPa, respectively[1–4] – has motivated a great deal of interest in CNT based nanocomposite materials.[5–10] Despite this significant scientific effort, the strength, modulus, and toughness of CNT based fibers and composites are typically dominated by weak shear interactions between adjacent shells, tubes, bundles, and matrix materials,[2,4,10,11] which has limited their application to hierarchical macroscopic composite materials. Here we demonstrate that the mechanical performance of double-walled nanotube (DWNT) bundles is greatly enhanced through high-energy electron-irradiation-induced shell–shell and tube–tube cross-linking. The effective tensile strength and elastic modulus are found to increase by an order of magnitude as compared to un-crosslinked bundles. This enhancement is attributed to covalent bonds formed between outer and inner DWNT shells as well as adjacent DWNT outer tubes within the bundle. Distinct failure mechanisms were also identified through in situ transmission electron microscopy (TEM) tensile tests of individual DWNT bundles revealing a sword-in-sheath like failure mechanism for low cross-linked bundles and complete fracture of all shells for highly cross-linked bundles. The optimized irradiation-induced cross-linking enhancements of DWNT bundles demonstraed here are predicted to translate to up to order-of-magnitude improvements in the mechanical behavior of advanced composites.

Engineering lateral interactions through cross-linking has become an essential tool in the development of advanced hierarchical composite materials, many of which are inspired by natural interfaces.[12–15] Successful hierarchical designs typically require both cross-linking to strong/stiff reinforcement elements (e.g. mineral crystals in the collagen fibrils in bone[14]) coupled with soft-sacrificial cross-linking (e.g. hydrogen bonding between beta-sheet crystals in spider silk[16]) between elements to enhance toughness.

In the case of individual CNTs and CNT bundles, one successful approach has been covalent cross-linking via high energy electron irradiation to increase effective strength and stiffness,[1,15,17–21] making them more attractive as reinforcement elements. Typically, irradiation with high energy particles is associated with introducing unwanted mechanical degradation, as is the case for high-energy x-ray irradiation of bone.[22] However, in the unique case of CNTs, controlled electron-irradiation has been predicted, and demonstrated experimentally, to yield significant improvements in the effective tensile modulus and strength of individual multi walled carbon nanotubes (MWNTs) by bridging intratube shells[1,15,20]–and the bending modulus of single wall carbon nanotube (SWNT) bundles–by bridging adjacent tubes.[17–19] The key element in irradiation improvements in CNT materials is that newly formed stiff cross-links, in particular Frenkel-pair defects between adjacent CNT shells,[1,23] facilitate load transfer to an inner core of material which is otherwise not mechanically utilized. This addresses the limitation of easy shear between shells and adjacent CNTs, which otherwise leads to order of magnitude reductions in the effective strength and elastic modulus of CNT based fibers (when the entire cross section of CNT shells is considered). While the intrinsic properties of CNT shells remains the same (or even slightly reduced due to newly formed defects) following irradiation, the effective mechanical properties such as modulus and strength are greatly enhanced as a result of cross-linking.

Theoretical models have predicted high effective strength of irradiated CNT bundles[19] and experiments have demonstrated irradiation improvements in strength for individual MWNTs;[1] however, experiments have yet to demonstrate the achievable strength of cross-linked SWNT or MWNT bundles. Reinforcement via cross-linking of MWNT bundles is a direction which is particularly advantageous, as compared to SWNT bundles, because MWNTs have a higher density of graphitic shells which can carry load if adequately cross-linked through both shell-shell and tube-tube bridges. In particular, double-wall carbon nanotubes (DWNTs) exhibit higher predicted strength and resistance to defects as compared to SWNTs.[15] Initial demonstrations of the advantages of small diameter MWNTs over SWNTs as reinforcements in composite materials have already been achieved both experimentally and theoretically.[11,15,24] When coupled to a matrix in composite materials, MWNTs can maintain high strength in their inner shells. This is in direct contrast to SWNTs, which exhibit strength reductions as the result of outer tube functionalization.[5] In addition, MWNTs are more resistant to irradiation-induced damage,[25] which may allow more controllable tuning of mechanical properties through a low density of intertube and intershell cross-links. Here, guided by previous experimental studies on MWNTs[1] and SWNT bundles,[17] we have investigated this effect on the effective tensile strength and elastic modulus of DWNT bundles as a result of cross-linking both adjacent shells and tubes via high-energy electron irradiation.

Dr. T. Filleter, R. Bernal, Prof. H. D. Espinosa
Department of Mechanical Engineering
Northwestern University
Evanston IL 60208–3111, USA
E-mail: espinosa@northwestern.edu
Dr. S. Li
NUANCE Center
Northwestern University
Evanston IL 60208–3111, USA

DOI: 10.1002/adma.201100547

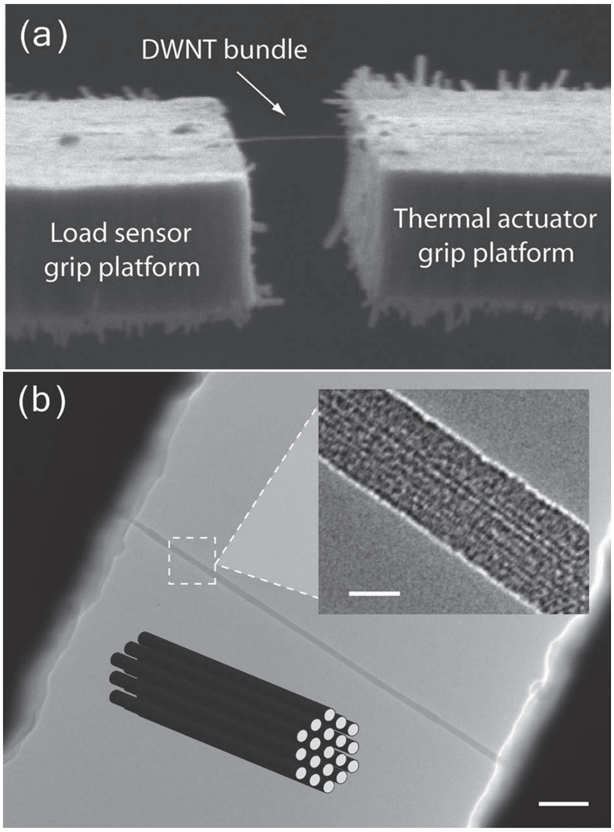

Figure 1. In situ TEM tensile testing of DWNT bundles. (a) SEM side view and (b) TEM top view images of a DWNT bundle suspended between the two grips of the MEMS based tensile testing device (Scale bar: 200 nm). (inset–upper right) High resolution TEM image of the suspended DWNT bundle (prior to irradiation) revealing a fringe pattern resulting from the hexagonally packed DWNTs within the bundle (Scale bar: 20 nm). (inset–lower left) Schematic representation of a DWNT bundle.

Figure 1a and b show electron microscope images of an isolated DWNT bundle suspended between the two gripping pads of a micro electromechanical (MEMS) testing system, described in detail in ref.[26–28] Care was taken during nanomanipulation to align the DWNT bundles with the tensile axis such that only bundles aligned within an angle of <15 degrees to the tensile axis (θ) were tested. The structure of isolated DWNTs was revealed through high resolution (HR) imaging before tensile tests (see inset Figure 1b). HR-TEM imaging of the bundle structure was hindered by vibration of the suspended structures as well as the low current density (<0.5 A/cm^2) used to reduce the minimum irradiation dose. Fringe patterns resulting from the hexagonally-packed DWNTs within bundles were observed and more clearly revealed through integration of perpendicular line scans across the diameter of the bundle. The isolated DWNT bundles were found to be uniform in diameter and structure, suggesting that they are composed of mostly continuous DWNTs bridging the entire tested region.

Isolated DWNT bundles exposed to controlled levels of 200 keV irradiation dose within a small range of diameter (11–28 nm) and length (~2–3 μm) were tested in situ TEM. The minimum irradiation dose required to image the specimen before and during a tensile test was determined to be ~0.5×10^{20} e/cm^2. Higher irradiation doses ($0.5–15.5 \times 10^{20}$ e/cm^2) were administered to the entire specimen by varying the total irradiation time before mechanical testing, at current densities between 0.3–0.5 A/cm^2. This range of irradiation dose was chosen in order to carefully probe the regime in which only a low density of cross-linking defects are induced in the bundle without introducing larger structural defects, which otherwise can significantly degrade its mechanical properties. Such an approach was motivated by molecular dynamic (MD) and molecular mechanics (MM) simulations of DWNTs, which have predicted maximum load transfer with only a small number of defects (~0.2–0.4 defects/Å).[1,20] Previous investigations of irradiation induced cross-linking in SWNT bundles focused on a range of dose in which the maximum increase in modulus was observed at the lowest controlled dose and subsequent irradiation reduced the modulus due to structural damage in CNTs as a result of large defects.[17] Here we have focused our investigation on the low dose regime in order to further characterize the onset of cross-link-stiffening and its effect on the tensile strength, tensile modulus, and failure mechanisms of DWNT bundles.

The structural and mechanical properties of each DWNT bundle tested in this study are summarized in **Table 1**. The bundle diameter was measured directly from high resolution TEM images (inset Figure 1b) and the number of fringes across

Table 1. Characteristics of DWNT bundles tested in situ TEM. Bundle diameter (d), length (l), number of fringes across the bundle diameter (N_f), total number of DWNTs within bundle (N_{DWNT}), angle of alignment with respect to the tensile loading axis (θ), effective tensile strength (σ), and effective tensile modulus (E).

Sample #	200 keV dose ($\times 10^{20}$ e/cm^2)	Diameter (nm)	Length (μm)	N_f	N_{DWNT}	θ (deg)	Tensile strength (GPa)	Tensile modulus (GPa)
1	0.5 ± 0.2	27.9	3.24	11	91	3.7	1.5	103 ± 19
2	2.87 ± 0.07	10.8	2.62	4	14	5.9	4.9	227 ± 9
3	6.0 ± 0.3	23.4	2.32	9	61	3.1	>5.3[a)]	483 ± 51
4	8.9 ± 0.3	13.7	2.77	5	19	10.8	10.7	693 ± 144
5	11.3 ± 0.3	15.2	2.55	6	30	13.4	17.1	355 ± 9
6	15.5 ± 0.4	17.5	3.25	7	37	2.3	12.8	498 ± 14

[a)] Sample 3 did not fail during the tensile experiment. Therefore, the maximum stress is given here as a lower limit for the effective tensile strength.

the diameter (N_f) was determined from integrating intensity profiles perpendicular to the bundle axis. The effective tensile modulus was determined from the linear region of the measured stress-strain responses where the effective stress was calculated by considering the entire cross-sectional area of all tubes and shells within an isolated bundle. The number of DWNTs in each bundle (N_{DWNT}) was determined by the measured value of N_f and considering a hexagonally packed circular geometry (for N_f odd: $N_{DWNT} = [3N_f^2 + 1]/4$, for N_f even: $N_{DWNT} = [3N_f^2 + 2N_f]/4$). The assumption of a regular hexagonal cross-sectional geometry was supported by both TEM bright-field images and electron energy loss spectroscopy (EELS) mapping. EELS measurements of a DWNT bundle revealed a thickness profile consistent with a regular cross-section (see Supporting Information). The cross-sectional area of each DWNT within a bundle was considered to be $A_{DWNT} = \pi\ (d_{in} + d_{out})\ t_{graphene}$ where d_{out} (2.2 nm) and d_{in} (1.6 nm) are the diameter of the outer and inner shells of each DWNT as determined from Raman spectroscopy[29] and $t_{graphene}$ is the thickness of a individual graphene layer (0.33 nm).

Figure 2a-b shows the stress-strain response of an irradiated DWNT bundle. The effective tensile modulus and tensile strength of DWNT bundles was found to significantly increase with increasing irradiation dose of 200 keV electrons to as high as 693 GPa and 17.1 GPa, respectively. These values are approximately one order of magnitude higher than un-irradiated DWNT bundles which were previously found to exhibit effective tensile modulus and effective tensile strength of 30–60 GPa and 2–3 GPa, respectively.[29] It should be noted that the mechanical properties of the un-irradiated DWNT bundles are consistent with previous studies of un-crosslinked CNT bundles and fibers.[17,18,30] Figure 2c and d show the dependence of effective tensile strength and tensile modulus on irradiation dose. Here, in contrast to SWNT bundles where only irradiation with lower energy electrons (80 keV) was effective at improving the bending modulus, controlled irradiation with 200 keV electrons is found to significantly improve the mechanical behavior of the DWNT bundles. In particular, this is to our knowledge the first demonstration of the high tensile strength of irradiated bundles. This improvement resulting from 200 keV irradiation is consistent with previous demonstrations which show that MWNTs are more resistant to high energy beam damage due to the presence of inner shells within each tube.[25] The effective tensile modulus is found to increase approximately

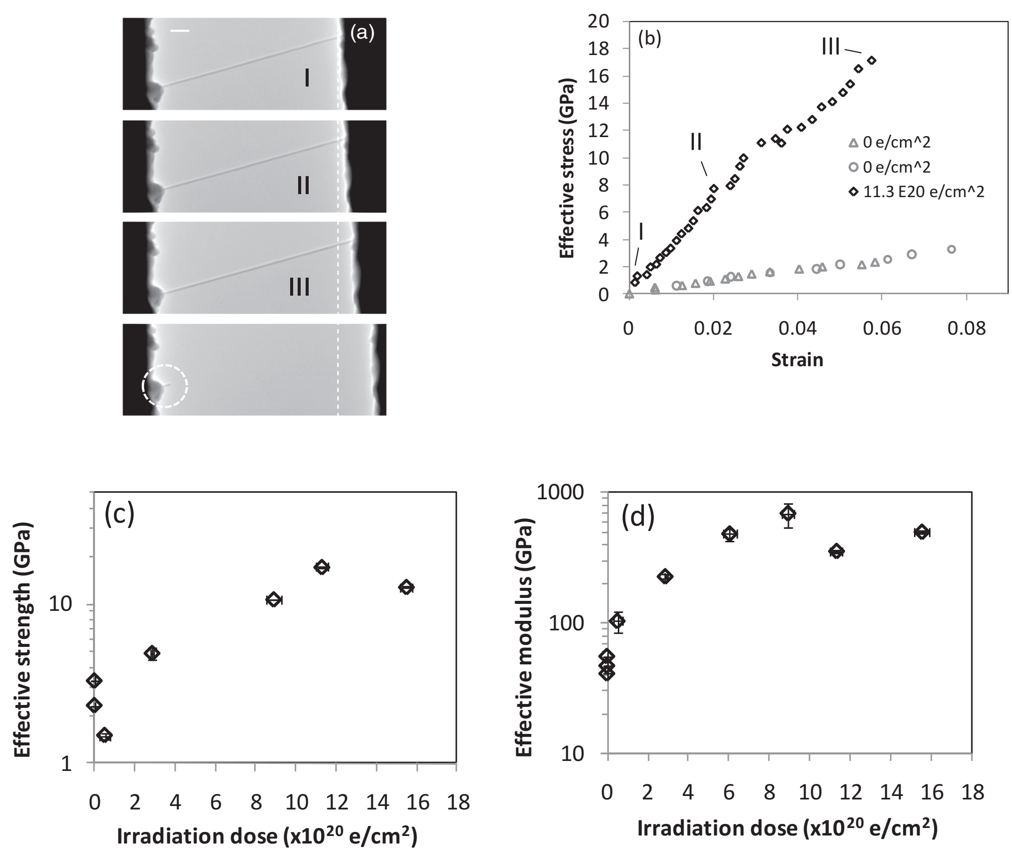

Figure 2. Electron irradiation induced increase in effective tensile strength and modulus of DWNT bundles. (a) Sequential images of a tensile test (I-III) conducted on a DWNT bundle in situ TEM. The bottom frame shows the remaining portion of the bundle after failure indicated by the circle. Scale bar: 200 nm. (b) Stress-strain curves of DWNT bundles irradiated with varying dose of 200 keV electrons. (c) Effective tensile strength and (d) effective tensile modulus as a function of irradiation dose. Results for 0 e/cm^2 were measured in situ SEM without exposure to 200 keV electrons (from[29] and analyzed here using the same model which considers the cross-sectional area of all tubes and shells within a bundle for calculating the effective stress.

linearly [slope = 72 GPa/(10^{20} e/cm^2)] with increasing irradiation dose up to doses as high as ~9×10^{20} e/cm^2. The increase is attributed to improved load transfer to inner tubes and shells facilitated by covalent cross-linking defects created during irradiation. Figure 2d demonstrated that the effective modulus of irradiated DWNT bundles approaches that of pristine individual CNTs (~1 TPa) before being reduced at higher irradiation due to an increased number of defects in the individual DWNTs consistent with observations of irradiation effects in SWNT bundles.[17] The effective strength also exhibits a similar dependence on irradiation dose reaching a maximum effective strength of 17.1 GPa at a dose of ~11×10^{20} e/cm^2. In this case, at lower doses, an approximately exponential increase in strength with increasing irradiation dose is observed (Figure 2c). The similar trends observed for both the effective modulus and strength in which there is an initial increases with dose, then a local maximum, and eventually a reduction is consistent with the following physical picture. At low irradiation dose, covalent cross-links form between shells within DWNTs and between adjacent tubes increasing the effective load bearing cross-section of the bundle which is then followed by an intrinsic degradation of the crystalline structure of DWNTs within the bundles for high irradiation doses as the structure becomes increasingly disordered. In addition to these changes in modulus and strength some reduction in failure strain is also observed with increasing radiation (Figure 2b).

High-resolution TEM images after failure reveal details of the different failure mechanisms of DWNT bundles exposed to varying levels of irradiation. **Figure 3**a shows the fracture surface of a bundle exposed to low irradiation (sample 1) after failure. A smaller inner bundle of DWNTs was found to pullout from the outer surrounding DWNTs upon failure. The low stiffness and strength of CNT bundles is typically attributed to such a sword-in-sheath failure mechanism in which the load is carried only by outer CNTs within a bundle, as has previously been observed in experiments on SWNT and DWNT bundles with in situ SEM.[29,31] Through in situ HR-TEM imaging, Figure 3 a demonstrates that the inner structure of the pulled out material is a well ordered smaller bundle of DWNTs. The regular packing of the pullout structure is confirmed by the fringe pattern observed in the pull out region (Figure 3c). In this case, an inner bundle with a fringe pattern of 4 DWNTs was pulled out of the larger bundle with a fringe pattern of 11 DWNTs upon failure (I and II in Figure 3). For sample 1, which was irradiated with a low dose, this demonstrates that before failure, the majority of the load was carried only by outer DWNTs within the bundle leading to a low effective tensile modulus. In contrast, sample 4, which was irradiated with a high dose, exhibited a completely fractured surface in which all shells and tubes of the DWNTs failed with minimal or no pullout (see Figure 3d). The HR-TEM image reveals that this bundle (sample 4) has a more irregular overall structure with an indication of a weak fringe pattern only near the center of the bundle due to a higher irradiation dose. This is consistent with the physical picture presented earlier in

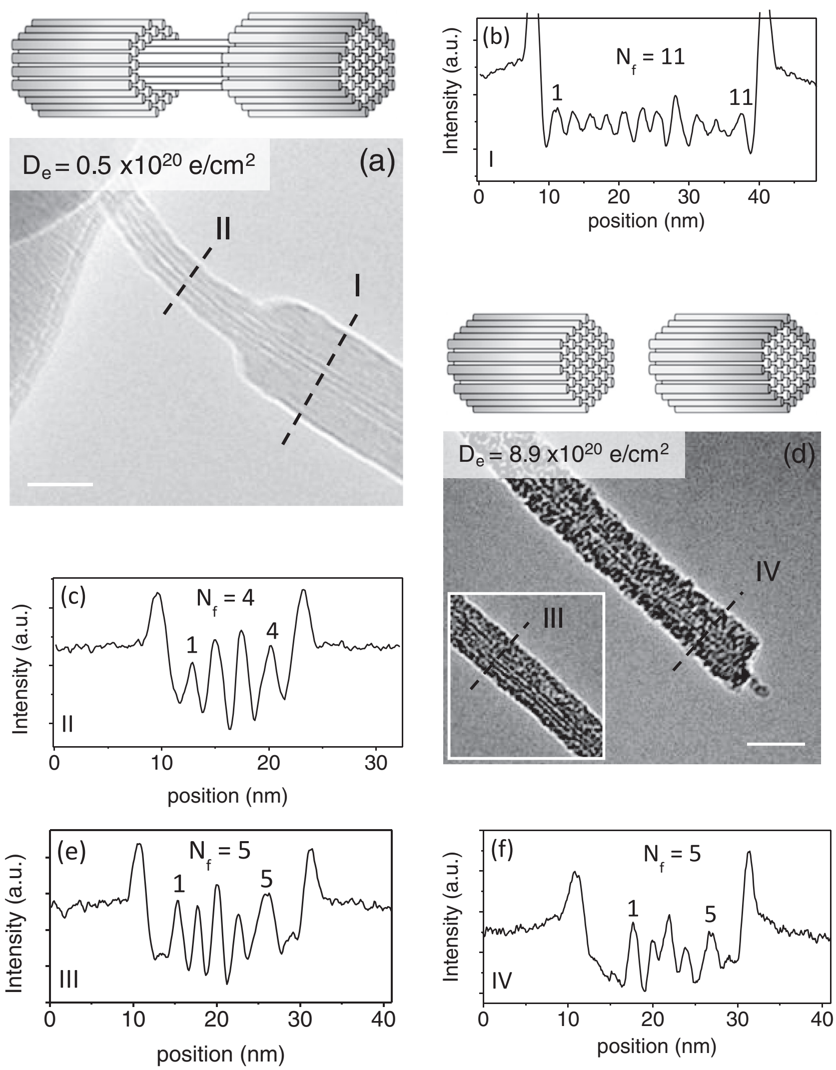

Figure 3. Distinct failure modes of DWNT bundles. (a) Sword-in-sheath failure of lightly irradiated sample: HR TEM image of fracture surface of the DWNT bundle (sample 1) after failure (Scale bar: 20nm). An inner bundle with four fringes is pulled out from the larger outer bundle. (b,c) Intensity profiles along lines indicated in (a) of inner and outer bundles revealing fringe patterns. Note: the two high intensity peaks present at the edges of each intensity profile result from TEM imaging of the bundle edges and do not represent fringes resulting from DWNTs within the bundle. The first and last of the inner fringes which result from DWNTs within each bundle are numbered for clarity. (d) Complete fracture of heavily irradiated sample: TEM image of DWNT bundle (sample 4) after failure (Scale bar: 20 nm). The inset shows the bundle prior to irradiation. (e,f) Intensity profiles along lines indicated in (b) revealing fringe patters before and after irradiation.

which the mechanical properties at higher irradiation dose are limited by the transformation to a more amorphous structure.

Next we will assess the potential impact of the observed cross-linking enhancements of DWNT bundles as reinforcement elements in nanocomposite materials. If applied as reinforcement elements in a polymer/CNT nanocomposite, the effective strength and modulus improvements in DWNT bundles demonstrated here could potentially translate to order of magnitude improvements in the resulting composite mechanical properties. Standard fiber composite models predict improvements in composite strength by up to 15x and composite modulus by up to 10x for typical polymer matrices when incorporating irradiation cross-linked DWNT bundles as reinforcement elements (see Supporting Information, Figure S2). In addition, irradiated DWNT based composites are predicted to exhibit significant improvements in strength (~1.5–3×) and modulus (~2.2×) as compared to advanced carbon-fiber/epoxy and CNT/carbon-fiber/epoxy composites,[32–34] which contain high volume fractions of MWNT/SWNTs, IM7, or AS4 carbon fiber reinforcement elements in an epoxy matrix (see Supporting Information, Figure S3).

In this work we have measured significant enhancements in the effective tensile strength and modulus of cross-linked DWNT bundles after irradiation with 200 keV electrons through in situ TEM tensile testing. Irradiated bundles were found to exhibit an effective tensile strength as high as ~17 GPa whereas the effective tensile modulus of irradiated bundles was found to increase by as much as 16 times that of un-crosslinked bundles to ~700 GPa approaching the tensile modulus of individual CNTs. A linear increase in effective tensile modulus and an exponential increase in effective tensile strength were observed for increasing dose of 200 keV electrons in the range of up to 9–11 × 10^{20} e/cm^2, demonstrating the ability to tailor the mechanical properties of CNT bundles in a low dose regime in which large defects are not playing a significant role. In addition to demonstrating the enhancement in mechanical properties for irradiated bundles, in situ TEM experiments also enabled the identification of the true load bearing cross-ection and revealed details of two distinct failure mechanisms in bundles with different cross-link concentration. In the case of low electron irradiation dose, a smaller inner bundle of DWNTs pulled out of the larger outer bundle upon initial failure resulting from easy shear between inner tubes in the absence of covalent cross-links, whereas heavily irradiated bundles exhibited complete fracture across all tubes and shells as a result of enhanced load transfer to inner tubes through covalent cross-links. The observed mechanical enhancement as a result of electron irradiation, coupled with the in situ TEM evidence of distinct failure mechanisms in the DWNT bundles, supports a physical picture in which covalent cross-links are formed between both shells within DWNTs and between adjacent tubes within bundles at low irradiation doses which increase the effective load bearing cross-section of the bundles and leads to significant improvements in both strength and modulus, whereas high irradiation doses leads to an intrinsic degradation of the crystalline structure of DWNTs within the bundles resulting in a limitation to the ultimate achievable improvements in the effective mechanical properties. The mechanical improvements as a result of high energy electron irradiation are also evidence of the beneficial robustness of DWNTs as compared to SWNTs for applications to nanocomposite materials. The developed fundamental understanding of the influence of multi-scale cross-linking on the mechanical behavior of reinforcement fibers, achieved here through irradiation induced covalent shell-shell and tube-tube cross-linking of DWNT bundles, can contribute to further the development of next-generation CNT hierarchical composite materials. In future work, one of the key challenges that remains to be studied will be the scaling of the demonstrated benefits of electron irradiation to macroscopic CNT fibers and composites. We envision that in the future covalently cross-linked CNT bundle reinforcement elements can be coupled together in a larger scale architecture, which also utilizes sacrificial bonds, to create high performance fibers, yarns, and composites with an exceptional combination of strength, stiffness, and toughness.

Experimental Section

Individual DWNT bundles were isolated from MER Corp. DWNT mats using a previously developed mechanical exfoliation technique.[29] Additional characterization of the DWNT bundles and mats (including HR-TEM, Raman spectroscopy, and thermogravimetric analysis) is described in detail in ref.[29] Tensile testing of individual DWNT bundles was performed using a micro electromechanical (MEMS) based testing system, described in detail in refs.[26–28] in situ a JEOL 2100F TEM operated at 200 kV. DWNT bundles were first fixed between the thermal actuator gripping pad and the load sensor gripping pad of the tensile testing device using a nanomanipulator (Klocke) and electron-beam induced deposition of carbon in situ SEM.[1] Tensile tests were then conducted by applying stepwise displacements to one end of the DWNT bundles (by increasing the current passing through the thermal acutator) and at each step measuring the force acting on the DWNT bundle. High resolution transmission electron microscope (HR-TEM) imaging of bundles allowed for both the direct measurement of strain during testing as well as a precise determination of the bundle thickness and structure prior to testing; a critical factor in determining the load bearing cross-sectional area of the bundles used in the determination of stress. The tensile force was determined from the calibrated stiffness (k_{LS} = 10.8 N/m) of the load-sensor beams and the measured deflection of the load sensor ($F = k_{LS}*d_{LS}$). The load sensor deflection (d_{LS}) at each step was determined by the difference between the applied displacement of the thermal actuator and the increase in the distance between gripping pads. HR-TEM images before testing were recorded with minimum beam exposure to avoid high irradiation dose (<0.3 × 10^{20} e/cm^2).

Supporting Information

Supporting Information is available from the Wiley Online Library or from the author.

Acknowledgements

HDE gratefully acknowledges support from ONR through award No. N00014–08-1–0108. The support and technical input provided by Dr. Ignacio Perez throughout the investigation is highly appreciated. The support from ARO through MURI award No. W911NF-09–1-0541 is also highly appreciated. The authors gratefully acknowledge Dr. A. Moravsky of MER Corp. for synthesis of the DWNT mat material and fruitful technical discussions. The authors also thank I. Petrov and E. Olson for their contribution in the development of the in situ TEM holder.

Received: February 11, 2011
Published online: April 29, 2011

COMMUNICATION

[1] B. Peng, M. Locascio, P. Zapol, S. Li, S. L. Mielke, G. C. Schatz, H. D. Espinosa, *Nat. Nanotechnol.* **2008**, *3*, 626
[2] M. F. Yu, B. S. Files, S. Arepalli, R. S. Ruoff, *Phys. Rev. Lett.* **2000**, *84*, 5552.
[3] M. F. Yu, O. Lourie, M. J. Dyer, K. Moloni, T. F. Kelly, R. S. Ruoff, *Science* **2000**, *287*, 637.
[4] J. P. Salvetat, G. A. D. Briggs, J. M. Bonard, R. R. Bacsa, A. J. Kulik, T. Stockli, N. A. Burnham, L. Forro, *Phys. Rev. Lett.* **1999**, *82*, 944.
[5] J. N. Coleman, U. Khan, W. J. Blau, Y. K. Gun'ko, *Carbon* **2006**, *44*, 1624.
[6] P. Ajayan, L. Schadle, C. Giannaris, A. Rubio, *Adv. Mater.* **2000**, *12*, 750.
[7] H. D. Wagner, O. Lourie, Y. Feldman, R. Tenne, *Appl. Phys. Lett.* **1998**, *72*, 188.
[8] W. Ding, A. Eitan, F. T. Fisher, X. Chen, D. A. Dikin, R. Andrews, L. C. Brinson, L. S. Schadler, R. S. Ruoff, *Nano Lett.* **2003**, *3*, 1593.
[9] A. A. Mamedov, N. A. Kotov, M. Prato, D. M. Guldi, J. P. Wicksted, A. Hirsch, *Nat. Mater.* **2002**, *3*, 190.
[10] J. N. Coleman, M. Cadek, R. Blake, V. Nicolosi, K. P. Ryan, C. Belton, A. Fonseca, J. B. Nagy, Y. K. Gunko, W. J. Blau, *Adv. Funct. Mater.* **2004**, *14*, 791.
[11] M. Cadek, J. N. Coleman, K. P. Ryan, V. Nicolosi, G. Bister, A. Fonseca, J. B. Nagy, K. Szostak, F. Be´guin, W. J. Blau, *Nano Lett.* **2004**, *4*, 353.
[12] M. J. Buehler, *Proc. Nat. Acad. Sci. USA* **2006**, *103*, 12285.
[13] M. J. Buehler, Y. C. Yung, *Nat. Mater.* **2009**, *8*, 175.
[14] H. D. Espinosa, J. E. Rim, F. Barthelat, M. J. Buehler, *Progr. Mater. Sci.* **2009**, *54*, 1059.
[15] E. M. Byrne, M. A. McCarthy, Z. Xia, W. A. Curtin, *Phys. Rev. Lett.* **2009**, *103*, 045502.
[16] S. Keten, Z. Xu, B. Ihle, M. J. Buehler, *Nat. Mater.* **2010**, *9*, 359.
[17] A. Kis, G. Csanyi, J. P. Salvetat, T. N. Lee, E. Couteau, A. J. Kulik, W. Benoit, J. Brugger, L. Forro, *Nat. Mater.* **2004**, *3*, 153.
[18] P. M. Ajayan, F. Banhart, *Nat. Mater.* **2004**, *3*, 135.
[19] J. A. Astrom, A. V. Krasheninnikov, K. Nordlund, *Phys. Rev. Lett.* **2004**, *93*, 4.
[20] A. F. Fonseca, T. Borders, R. H. Baughman, K. Cho, *Phys. Rev. B* **2010**, *81*, 045429.
[21] M. Terrones, F. Banhart, N. Grobert, J.-C. Charlier, H. Terrones, P. M. Ajayan, *Phys. Rev. Lett.* **2002**, *89*, 075505.
[22] H. D. Barth, M. E. Launey, A. A. MacDowell, J. W. A. III, R. O. Ritchie, *Bone* **2010**, *46*, 1475.
[23] K. Urita, K. Suenaga, T. Sugai, H. Shinohara, S. Iijima1, *Phys. Rev. Lett.* **2005**, *94*, 155502.
[24] X. Sui, D. Wagner, *Nano Letters* **2009**, *9*, 1423.
[25] A. V. Krasheninnikov, K. Nordlund, *J. Appl. Phys.* **2010**, *107*, 071301.
[26] Y. Zhu, H. D. Espinosa, *Proc. Nat. Acad. Sci. USA* **2005**, *102*, 14503.
[27] H. D. Espinosa, Y. Zhu, N. Moldovan, *J. Microelectromech. Syst.* **2007**, *16*, 1219.
[28] Y. Zhu, N. Moldovan, H. D. Espinosa, *Appl. Phys. Lett.* **2005**, *86*, 013506.
[29] M. Naraghi, T. Filleter, A. Moravsky, M. Locasio, R. O. Loufty, H. D. Espinosa, *ACS Nano* **2010**, *4*, 6463.
[30] A. B. Dalton, S. Collins, E. Munoz, J. M. Razal, V. H. Ebron, J. P. Ferraris, J. N. Coleman, B. G. Kim, R. H. Baughman, *Nature* **2003**, *423*, 703.
[31] M. F. Yu, B. Files, S. Arepalli, R. Ruoff, *Phys. Rev. Lett.* **2000**, *84*, 5552.
[32] I. M. Daniel, O. Ishai, *Engineering Mechanics of Composite Materials*, Oxford University Press, **2006**.
[33] E. Bekyarova, E. T. Thostenson, A. Yu, H. Kim, J. Gao, J. Tang, H. T. Hahn, T.-W. Chou, M. E. Itkis, R. C. Haddon, *Langmuir* **2007**, *23*.
[34] E. Bekyarova, E. T. Thostenson, A. Yu, M. E. Itkis, D. Fakhrutdinov, T.-W. Chou, R. C. Haddon, *J. Phys. Chem. C* **2007**, *111*, 17865.